Materials Science-Poland, 35(3), 2017, pp. 470-478
http://www.materialsscience.pwr.wroc.pl/
DOI: 10.1515/msp-2017-0063

DE GRUYTER OPEN

Structural, optical and electrical characterization of CBD synthesized CdO thin films: influence of deposition time

M.R. DAS, A. MUKHERJEE, P. MITRA*

Dept. of Physics, The University of Burdwan, Golapbag, Burdwan-713104, India

Cadmium oxide (CdO) thin films were grown on glass substrates by chemical bath deposition (CBD) method for different deposition times using cadmium acetate as cationic precursor. The structural and optical characterization was carried out using XRD, TEM, and UV-Vis spectrophotometer measurements. Structural analyses with XRD confirmed cubic structure of the CdO. Average particle size estimated from Rietveld refinement method of XRD pattern corresponded well with TEM measurement. The optical band gap varied between 2.35 eV to 2.48 eV with deposition time and an increase in optical band gap with decreasing film thickness was observed. The AC electrical conduction behavior of the CdO film was investigated as a function of temperature as well as frequency. The conductivity measurements indicated localized conduction and hopping of carriers between localized states. The value of real part of dielectric constant was found to decrease with frequency and increase with temperature. The Nyquist plots at different temperatures showed the existence of both grains and grain boundaries contributing to conduction mechanism.

Keywords: *chemical bath deposition (CBD); CdO thin film; XRD; band gap; AC conductivity*

1. Introduction

Transparent conducting oxides (TCOs), in recent years, have attracted the attention of many researchers due to their unique physical properties and wide range of applications in industry. Cadmium oxide (CdO) is a type of transparent conducting oxide (TCO) material that possesses both high electrical conductivity and high optical transparency in the visible region of electromagnetic spectrum. CdO is an n-type semiconductor with a wide direct optical band gap of ∼2.2 eV [1] that exhibits rock salt structure (FCC). Thin films of CdO find wide applications in solar cells, smart windows, optical communications, flat panel displays, phototransistors, as well as other types of applications like IR heat mirror, gas sensors, low-emissive windows, thin-film resistors, etc. [2–5].

Many physical and chemical techniques such as pulsed laser deposition [6, 7], RF magnetron sputtering [8], DC magnetron reactive sputtering [9], metal organic chemical vapor deposition [10, 11], vacuum evaporation [12], electron beam evaporation [13], spray pyrolysis [14, 15], electrodeposition [16], sol-gel [16, 17], chemical bath deposition (CBD) [19, 20] and modified CBD (also termed as successive ionic layer adsorption and reaction or SILAR) [21], etc. have been used in order to obtain CdO thin films. Among the chemical techniques, CBD, also known as CSD (chemical solution deposition) has many advantages such as low cost and convenience to carry out on a variety of substrates. CBD also offers high growth rate at low temperature and control of shape and size of thin films. The thickness of the deposited layers may be readily controlled by variation of the deposition time making the process suitable for large area processing at low fabrication cost. Although CBD has been widely used by many researchers to deposit thin films of CdO, primarily cadmium chloride [19, 20, 22, 23] and cadmium sulfate [24, 25] have been used as a source of cations. This always introduces the possibility of chlorine and sulfur incorporation into the films. In this work, CdO thin films were deposited on glass substrates using cadmium acetate as a source of cation with the objective to prepare chlorine and sulfur free thin films of CdO. The influence of deposition time (thickness)

*E-mail: mitrapartha1@rediffmail.com

© 2017. This is an open access article distributed under the Creative Commons Attribution-NonCommercial-NoDerivatives 3.0 License.
(http://creativecommons.org/licenses/by-nc-nd/3.0/)

on structural properties and optical band gap has been studied. In order to get a detailed idea about the dynamics of mobile ions, AC conductivity measurements have been carried out for CdO thin films, probably for the first time. The results have been analyzed with a view of understanding the conduction mechanism involved.

2. Experimental

Cadmium oxide thin films were deposited on microscopic glass substrates using CBD technique. Before deposition, the substrates were ultrasonically cleaned with detergent and ethanol. Finally, they were rinsed with distilled water and dried in an oven. Cadmium acetate [$Cd(CH_3COO)_2$] was used as cationic precursor solution (source of Cd^{2+} ion). 4 mL of 1 M [$Cd(CH_3COO)_2$] was taken in a beaker and ammonia solution (NH_4OH) was added to it as a complexing agent. The solution volume was fixed at 50 mL by adding deionized water. Ammonia addition was carried out under continuous stirring with a magnetic stirrer and pH of the solution was measured by a digital pH meter. When the solution pH was 11.5, the cleaned substrate was immersed vertically in the solution. The substrate was taken out from the solution after a suitable time. It was then washed with distilled water and dried. Three samples with deposition times of 24 h, 26 h and 48 h were prepared. White film of cadmium hydroxide that was formed on the substrate, was subsequently converted to cadmium oxide by heating in air at 300 °C for two hours.

Phase identification and crystalline properties of the samples were studied by X-ray diffraction (XRD) method with the help of a Bruker (D8 advance) X-ray diffractometer using Ni-filtered CuKα radiation ($\lambda = 1.5418$ Å). The diffraction data were recorded in the range of 20° to 70° scattering angle and the experimental peak positions were compared with standard Joint Committee of Powder Diffraction System (JCPDS) files. Rietveld refinement method [26, 27] was used to determine the particle size. For further characterization, transmission electron microscopy (TEM) investigation was carried out using JEOL JEM-1400 Plus microscope operating at 120 kV. The sample was detached from the substrate by immersion in ethanol ultrasonic bath, mounted on a carbon coated copper grid, dried, and used for TEM measurements. UV-Vis spectrophotometric measurements were taken using a double-beam spectrophotometer (Shimadzu UV-1800) at room temperature. The spectra were recorded by using a similar glass as a reference and hence, the absorption resulting from the film only was obtained. The band gap of the films was calculated from the absorption edge of the spectrum. Impedance measurements were carried out in the frequency range of 100 Hz to 2 MHz using Agilent high precision LCR meter (Keysight E4980A). Direct measurement of DC conductivity of the samples is often not possible because of the polarization effects at the sample-electrode interface and difficulties in finding a suitable electrode. Accordingly, the AC impedance plots were used to find the bulk resistance and DC conductivity was obtained using the relation:

$$\sigma_{dc} = \frac{d}{RA} \tag{1}$$

where d is the thickness of the sample, A is the area of cross-section of the sample and R is the bulk resistance obtained from impedance analysis. AC conductivity was determined using the relation:

$$\sigma(\omega) = G_p(\omega)d/A \tag{2}$$

where $G_p(\omega)$ is the conductance. The thickness d of the films was measured by the weight difference-density consideration [28, 29] using an electronic high-precision balance. The thickness of the film was found to increase with deposition time. The film deposited for 24 h was ~320 nm and that deposited for 48 h was ~810 m.

3. Results and discussion

Fig. 1 shows the XRD patterns of CdO thin films deposited for different deposition times along with the Rietveld fitting outputs. The difference plot, i.e. the residual of fitting ($I_o - I_c$) between the observed I_o and fitted pattern I_c is shown

at the bottom of Fig. 1 below the respective patterns. An appropriate fit (continuous line) has been observed with the GoF's and in all cases it was lying between 1.22 and 1.28, signifying that the fitting equations are good enough for all experimental patterns. The diffraction peaks observed at ∼33.16°, ∼38.41°, 55.52°, 66.05° and 69.46°, respectively can be associated with cubic cadmium oxide (JCPDS file No. 05-0640). The corresponding diffraction planes are (1 1 1), (2 0 0), (2 2 0), (3 1 1) and (2 2 2), respectively. The reduction of the width of the diffraction peaks with increasing deposition time clearly indicates an increase in particle size. The average value of particle size estimated from Rietveld refinement method is ∼13.4 nm, ∼23.6 nm and ∼40.1 nm for 24 h, 36 h and 48 h deposited films, respectively. Lattice strain estimated from the refinement method was found to decrease with deposition time. Its value was $\sim 3.53 \times 10^3$, $\sim 2.32 \times 10^3$ and $\sim 1.72 \times 10^3$ for 24 h, 36 h, and 48 h deposited films, respectively indicating better quality of the film deposited for higher deposition time. The error margins on both grain size and strain were within ±5 %. It seems that with an increase in deposition time, the number of ions contributing to the film formation process increases at a faster rate. This is also evident from the thickness value which shows higher growth rate for 48 h deposited film compared to 24 h deposited film. Higher value of microstrain in thinner film also implies presence of pores and higher density of defect states compared to thicker film. The reacting ions arriving at the substrate-solution interface reach the nuclei which are already growing and thus reduce the defect state density.

The indexed selected area electron diffraction (SAED) pattern of CdO synthesized after 36 hours of deposition is shown in Fig. 2a. The first diffraction ring in the SAED pattern is due to (1 1 1) reflection and the second one is due to (2 0 0) reflection. Low magnification TEM image is shown in Fig. 2b. The observed average particle size of ∼25 nm correlates well with X-ray value. The histogram of particle size distribution is shown in Fig. 2c.

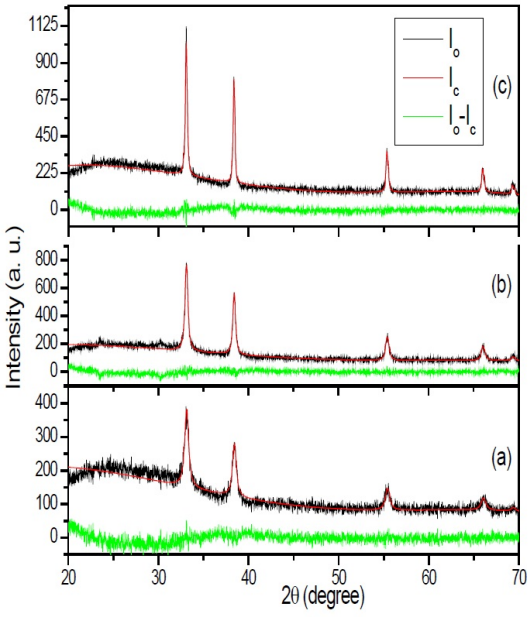

Fig. 1. Observed I_o and fitted I_c X-ray powder diffraction patterns of CdO thin films deposited for (a) 24 h, (b) 36 h and (c) 48 h.

Band gap energy E_g was derived from the mathematical treatment of the data obtained from the absorbance vs. wavelength spectrum in the wavelength range of 475 nm to 975 nm for direct band gap CdO [30] using the following relationship:

$$(\alpha\hbar\nu)^2 = A(\hbar\nu - E_g) \tag{3}$$

where ν is frequency, A is a function of index of refraction and hole/electron effective masses, ħ is the Planck constant. Curves (a), (b) and (c) in Fig. 3 show the plot of absorbance as a function of wavelength for different deposition times. Fig. 4 shows the plot of $(\alpha\hbar\nu)^2$ as a function of photon energy ħν. Extrapolation of the line to the base line, where the value of $(\alpha\hbar\nu)^2$ is zero, gives the value of band gap E_g. The value of the band gap was found to decrease with increasing thickness (deposition time). The observed values were ∼2.48 eV, ∼2.41 eV and ∼2.35 eV for 24 h, 36 h and 48 h deposited films, respectively. The band gap values were an average of three measurements in different areas of the film. There was a discrepancy of ∼0.02 eV in the measured values. The observed result suggests a decrease in optical band gap

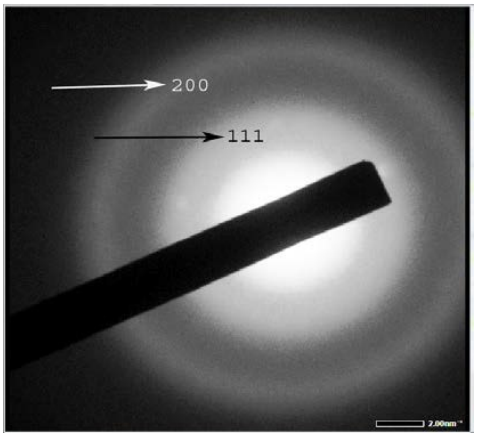

(a)

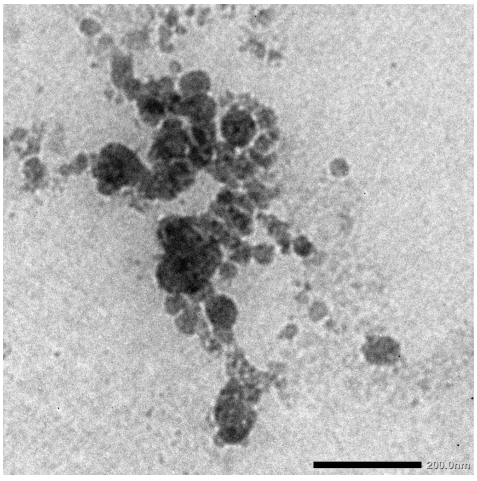

(b)

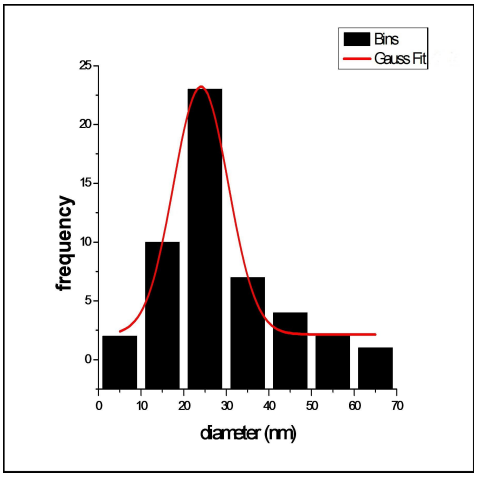

(c)

Fig. 2. Selected area electron diffraction (SAED) image of 24 h deposited CdO; (b) low magnification TEM image; and (c) histogram of particle size distribution.

with increasing deposition time, i.e. increasing film thickness or conversely, an increase in optical band gap with decreasing film thickness. Although no such report on CdO thin films has been reported in the literature to the best of our knowledge, such an observation indicating an increase in disorder with decreasing thickness has been reported for other binary and ternary semiconducting materials [31–33]. This may be attributed to introduction of some defects which creates localized states in the band gap. With decreasing thickness, unsaturated bonds can be produced as a result of an insufficient number of atoms [31–34]. These bonds are responsible for the formation of some defects in the films and these defects produce localized states in the films. The thicker film increases the width of localized states in the optical band gap, consequently, the optical absorption edge decreases with reverse effect.

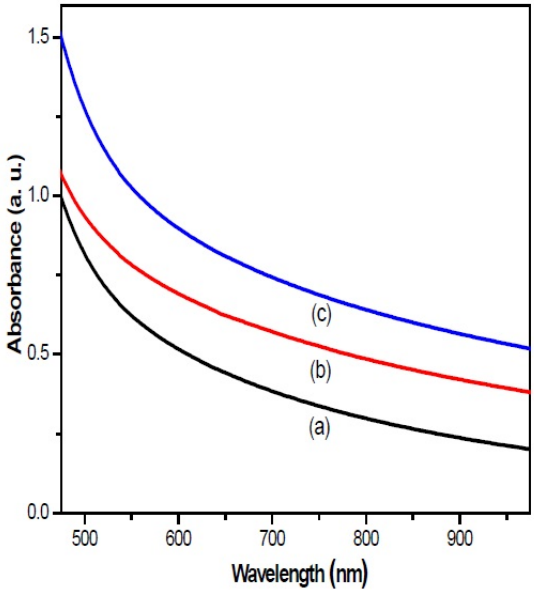

Fig. 3. Absorbance versus photon wavelength of CdO thin films deposited for (a) 24 h, (b) 36 h and (c) 48 h.

The AC electrical conduction behavior of CdO film was investigated as a function of temperature as well as frequency. The AC conductivity of CdO thin films was measured in the frequency range of 100 Hz to 2 MHz by varying the temperature from 548 K to 673 K. The variation of AC

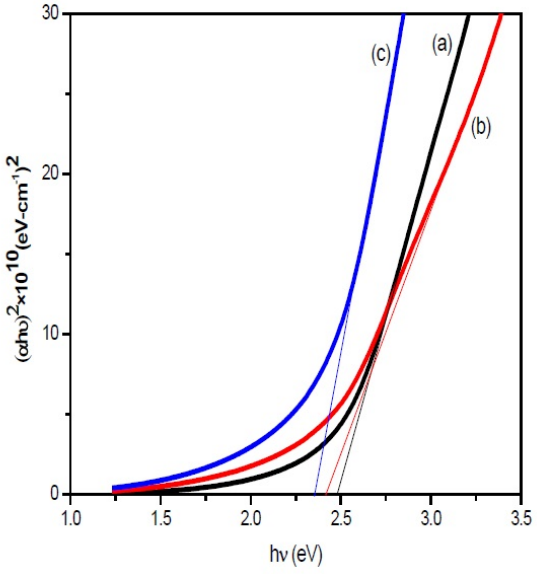

Fig. 4. Plots of $(\alpha\hbar\nu)^2$ versus photon wavelength for CdO thin films deposited for (a) 24 h, (b) 36 h and (c) 48 h.

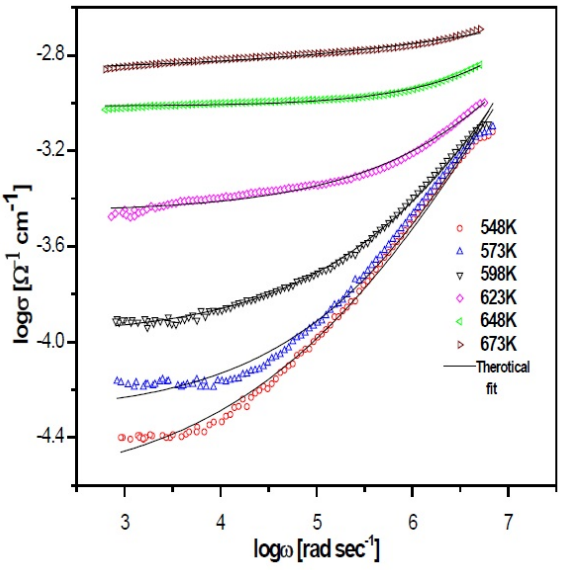

Fig. 5. Variation of AC conductivity of CdO thin film deposited for 36 h as a function of frequency at different temperatures.

conductivity with frequency for 36 h deposited film is shown in Fig. 5. The figure shows the frequency dependence of AC conductivity at different fixed temperatures on a log-log scale. It is evident from the figure that the AC conductivity is nearly constant at low frequencies for all temperatures. Above a certain frequency, it increases with an increase in frequency. This type of variation indicates localized conduction. Contrary to this, in case of free band conduction the AC conductivity decreases with frequency [35]. Also, the AC conductivity is found to increase with an increase in temperature. This rise of AC conductivity with temperature might be due to thermal activation which allows the hopping of carriers between different localized states. Thus, the increase in AC conductivity with the increase in temperature and frequency clearly indicates mobile charge carriers responsible for hopping. According to Jonscher [36], the origin of frequency dependence of conductivity lies in the relaxation phenomena arising due to mobile charge carriers. When the mobile charge carrier hops to a new site from its original position, it remains in a state of displacement between two potential energy minima which includes contributions from other mobile defects.

The AC conductivity follows the Almond-West relation [37]:

$$\sigma(\omega) = \sigma_{dc}[1 + \omega/\omega_H{}^n] \tag{4}$$

where ω is the angular frequency, ω_H is the hopping or crossover frequency from where the conductivity starts to disperse, σ_{dc} is the DC value of conductivity and n is the frequency exponent. The frequency exponent n, DC conductivity and hoping frequency were obtained from the least square fits of the data with equation 4. It was found that the value of n lies between 0 and 1 and it decreases with temperature. The temperature dependence of n indicates the hopping conduction. The hoping frequency is found to increase with temperature which means the higher temperature hoping of the mobile charge occurs at higher value of frequency.

The variation of AC conductivity with frequency for 24 h, 36 h and 48 h deposited films at the temperature of 598 K is shown in Fig. 6. The figure shows the frequency dependence of AC conductivity with frequency on a log-log scale. It was found that the value of conductivity increases with an increase of deposition time. This is because

there are number of aggregated particles with lots of insulating gaps in thinner films. As the deposition time increases, the thickness and grain size increase causing that the islands of aggregated particles transform into a continuous band. So, the insulating gaps are minimized thus decreasing the resistivity, i.e. increasing the conductivity.

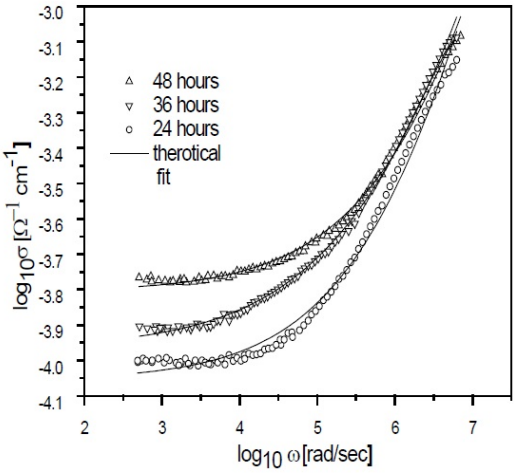

Fig. 6. Variation of AC conductivity of CdO thin films deposited for (a) 24 h, (b) 36 h and (c) 48 h.

Fig. 7 shows the graph of $\log\sigma_{dc}$ versus 1000/T which confirms the semiconducting nature of CdO as DC conductivity increases with temperature. It is also observed from the graph that the conductivity increases with the thickness which might be due to a decrease in grain boundaries with an increase of film thickness as reported previously [38]. The obtained data was fitted to the Arrhenius equation:

$$\sigma_{dc} = \sigma_0 \exp\left(-\frac{E_a}{kT}\right) \tag{5}$$

where σ_0 is the pre-exponential factor, E_a is the activation energy for the DC conduction process and k is the Boltzmann constant. The values of activation energy E_a were calculated from the slopes of $\log\sigma_{dc}$ versus 1000/T plots. The calculated values of activation energy are ~0.235 eV, ~0.266 eV and ~0.312 eV for 24 h, 36 h and 48 h deposited films, respectively, indicating enhancement of activation energy with increasing film thickness. This value of thermal activation energy is much less than the actual band gap value and thus it represents the location of trap states below the conduction band. This further suggests that the conduction in the material is due to thermally assisted tunneling of the charge carriers through the grain boundary barrier and transition from donor level to conduction band. The change of activation energy may be due to differences in deposition time, fabrication process and other growth parameter [39, 40].

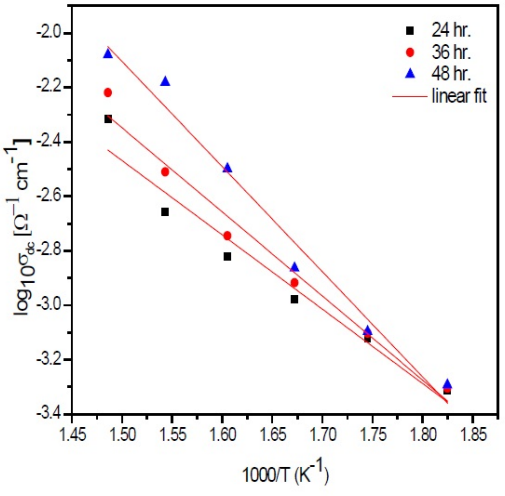

Fig. 7. Plots of $\log_{10}\sigma_{dc}$ versus 1000/T (Arrhenius plot of the DC conductivity) of CdO thin films deposited for 24 h, 36 h and 48 h.

Variation of the real part of dielectric constant, $\epsilon_1(\omega)$ with frequency at different temperatures is shown in Fig. 8. It can be seen that the dielectric constant $\epsilon_1(\omega)$ decreases with increasing frequency at a constant temperature, while it shows an increasing trend with increasing temperature at a constant frequency. The decrease of dielectric constant with frequency can be explained by the fact that at higher frequencies, the dipoles cannot align themselves and the contribution of polarization to the dielectric constant becomes negligible [41, 42]. On the other hand, the increase of dielectric constant with temperature can be explained by the fact that the bound charge carriers get gradually a higher amount of thermal excitation energy to be able to respond to the change in the external field more easily [43]. Finally, at higher frequencies,

the electronic polarization is dominant and the real part of dielectric constant becomes constant.

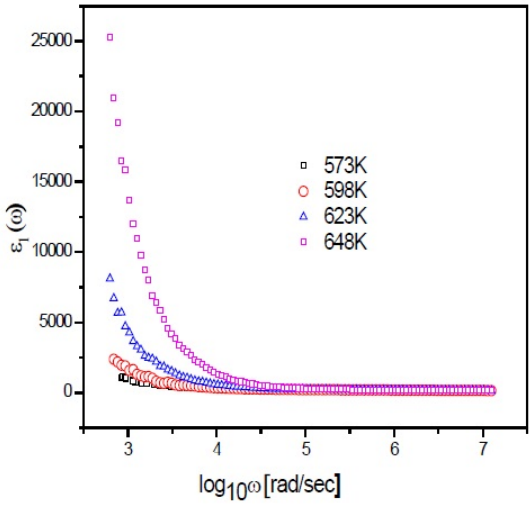

Fig. 8. Variation of real part of dielectric constant of CdO thin films deposited for 48 h with frequency at different temperatures.

The plot of real part Z′ and imaginary part Z″ of complex impedance (Nyquist plot) at different temperatures for the 48 h deposited film is shown in Fig. 9. These plots are a very powerful technique for the characterization of electrical behavior. Fig. 9 shows the Nyquist plot of the sample at selected temperatures. The Nyquist plot is characterized by semicircular arcs whose diameters decrease with an increase of temperature. A single arc represents one source of possible resistance while the charge carriers move or hop through the lattice structure of the material. The impedance spectrum of the sample shows a depressed semicircle which could not be fitted with the equation of a single semicircle thus indicating the presence of both grain resistance R_g and grain boundary resistance R_{gb} in the material. In order to separate out the bulk (grain) and grain boundary contributions to the total conductivity, they were fitted by EC lab software using an equivalent circuit. The equivalent circuit may be considered as two parallel RC elements connected in series [44], as shown in the inset of Fig. 9 where C_g denotes grain capacitance and C_{gb} denotes grain boundary capacitance. R_g and R_{gb} represent grain and grain boundary resistances respectively. The values of R_g, R_{gb}, C_g and C_{gb}, which were obtained from fitting the experimental data with two semicircular equations, are shown in Table 1. It is evident that grain (bulk) resistance is lower than the grain boundary resistance. Such an observation is expected in thin films where conductivity is controlled primarily by grain boundaries [45]. The decrease in resistance with an increase in temperature suggests semiconducting behavior of the CdO film. In addition to this, the intercept of the arc on the real axis shifts toward the origin of the complex plane with increasing temperature. This shift means a reduction of the resistive behavior of the sample caused by grain boundary conduction i.e. lowering of barrier to the mobility of charge carriers, aiding electrical conduction with the rise in temperature.

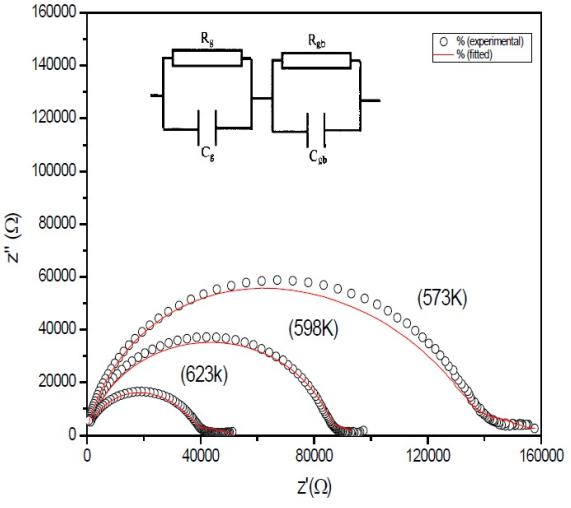

Fig. 9. Plots of Z″ versus Z′ (complex impedance spectra) at different temperatures for CdO thin films deposited for 48 h.

4. Conclusions

Phase pure CdO thin films were synthesized by CBD technique using cadmium acetate as cationic precursor probably for the first time. The use of cadmium acetate removed the possibility of chlorine or sulfur ion incorporation in the synthesized films compared to cadmium chloride and cadmium

Table 1. The values of resistance and capacitance of CdO thin films deposited at different temperatures.

Compound name	Temperature [K]	R_{gb} [Ω]	R_g [Ω]	C_{gb} [V]	R_g [F]
CdO	573	∼132610	∼7440	$\sim 6.00 \times 10^{-13}$	$\sim 1.07 \times 10^{-11}$
	598	∼81450	∼5535	$\sim 9.77 \times 10^{-13}$	$\sim 1.43 \times 10^{-11}$
	623	∼34490	∼4535	$\sim 23.1 \times 10^{-13}$	$\sim 1.75 \times 10^{-11}$

sulfate baths, primarily used by researchers. Polycrystalline cubic CdO with particle size depending on deposition time was observed. The average value of particle size estimated from Rietveld refinement of XRD pattern was ∼13.4 nm, ∼23.6 nm and ∼40.1 nm for 24 h, 36 h and 48 h deposited films, respectively and it corresponded well with TEM measurement. The density of defect states in the films decreased with enhanced film thickness which was evidenced by the decrease in microstrain for thicker films. The optical band gap was found to decrease with increasing deposition time. The values were ∼2.48 eV, ∼2.41 eV and ∼2.35 eV for 24 h, 36 h and 48 h deposited films respectively. This might be due to introduction of defects in thinner films which created localized states in the band gap. Both structural and optical studies indicated improved crystallinity in the film with enhanced deposition time. AC conductivity measurement indicated localized conduction and hopping of carriers between localized states. DC conductivity result showed the existence of such localized states below the conduction band. The Nyquist plots at different temperatures showed the impact of both grain (bulk) and grain boundaries in the conduction mechanism with grain boundary resistance being the dominant one.

Acknowledgements

One of the authors (M.R. Das) wishes to thank the University Grants Commission, India, for awarding him a fellowship during the tenure of the work. The authors acknowledge S. Bandyopadhyay, Dept. of Physics, The University of Burdwan, for the AC conductivity measurements.

References

[1] HENRIGUEZ R., GREZ P., MUNOZ E., LINCOT D., DALCHIELE E.A., MAROTTI R., GOMEZ H., *Sci. Technol. Adv. Mat.*, 9 (2008), 025016.

[2] CALNAN S., TIWARI A.N., *Thin Solid Films*, 518 (2010), 1839.

[3] AZARIAN A., IRAJI A., MAHDAVI S.M., *Int. J. Nanotechnol.*, 6 (2009), 997.

[4] ZHAO Z., MOREL D.L., FEREKIDES C.S., *Thin Solid Films*, 413 (2002), 203211.

[5] DAKHEL A.A., *Adv. Optoelectron.*, 2013 (2013), 1.

[6] GUPTA R.K., GHOSH K., PATEL R., KAHOL P.K., *J. Alloy. Compd.*, 509 (2011), 4116.

[7] GUPTA R.K., GHOSH K., PATEL R., MISHRA S., KAHOL P., *Mater. Lett.,* 62 (2008), 4103.

[8] SAHA B., THAPA R., CHATTOPADHYAY K.K., *Sol. Energ. Mat. Sol. C.*, 92 (2008), 1077.

[9] SUBRAMANYAM T., KRISHNA B., UTHANNA S., NAIDU B., REDDY P., *Vacuum*, 48 (1997), 565.

[10] LI X., GESSERT T., COUTTS T., *Appl. Surf. Sci.*, 223 (2004), 138.

[11] ELLIS D., IRVINE S., *J. Mater. Sci. Mater. El.*, 15 (2004), 369.

[12] DAKHEL A.A., *J. Alloy. Compd.*, 475 (2009), 51.

[13] ALI H., MOHAMED A., WAKKAD M., HASANEEN M., *J. Appl. Phys.*, 48 (2009), 041101.

[14] JUSEO D., *J. Korean Phys. Soc.*, 45 (2004), 1575.

[15] JEYAPRAKASH B.G., KESAVAN K., KUMAR A., MOHAN S., AMALARANI A., *J. Am. Sci.*, 6 (2010), 75.

[16] ABDULRIDHA M.S., *IJNC*, 2 (2016), 21.

[17] BARI R.H., *IJOCC*, 1 (2015), 136.

[18] SERBETCIA Z., GUNDUZB B., GHAMDIC A.A., HAZMIC F., KA K., TANTAWYD F., YAKUPHANOGLUC F., FAROOQ F.A., *Acta Phys. Pol. A*, 126 (2014), 798.

[19] EZEKOYE B.A., EZEKOYE V.A., OFFOR P.O., UTAZI S.C., *IJPS*, 8 (2013), 1597.

[20] LALITHAMBIKA K.C., SHANTHAKUMARI K., SRIRAM S., *Int. J. ChemTech Res.*, 6 (2014), 3071.

[21] SALUNKHE R.R., DHAWALE D.S., GUJAR T.P., LOKHANDE C.D., *Mater. Res. Bull.*, 44 (2009), 364.

[22] BUBA D.A., SAMSON D.O., *Int. J. Curr. Res. Aca. Rev.*, 3 (2015), 116.

[23] PERUMAL P., MANOHARI A.G., VALANARASU S., KATHALINGAM A., RHEE J., SOUNDARAM N., CHANDRAMOHAN R., *JESMAT*, 2 (2012), 71.

[24] KHALLAFA H., CHEN C., CHANG L., LUPAN O., DUTTA A., HEINRICHA A., SHENOUDA A., CHOW L., *Appl. Surf. Sci.*, 257 (2011), 9237.

[25] KAWAR S.S., *IJCPS*, 1 (2012), 11.

[26] RIETVELD H.M., *J. Appl. Crystallogr.*, 2 (1969), 65.

[27] SAIN S., PARTA S., PRADHAN S. K., *Mater. Res. Bull.*, 47 (2012), 1062.

[28] MITRA P., KHAN J., *Mater. Chem. Phys.*, 98 (2006), 279.
[29] KALE S.S., MANE R.S., PATHAN H.M., SHAIKH A.V., JOO O.S., HAN S.H., *Appl. Surf. Sci.*, 253 (2007), 4335.
[30] ORTEGA M., SANTANA G., ACEVEDO A.M., *Solid State Electron.*, 44 (2000), 1765.
[31] RABEH M.B., KHEDMI N., FODHA M.A., KANZARI M., *Energy Procedia*, 44 (2014), 52.
[32] SONMEZOGLU S., ARSLAN A., SERIN T., SERIN N., *Phys. Scr.*, 84 (2011), 065602.
[33] VARNAMKHASTI M.G., FALLAH H.R., MOSTAJABODDAVATI M., HASSANZADE M., *Vacuum*, 86 (2012), 131.
[34] OVSHINSKY S.R., ADLER D., *Contemp. Phys.*, 19 (1978), 109.
[35] ANWAR M., HOGARTH C.A., *J. Mater. Sci.*, 25 (1990), 3906.
[36] JONSCHER A.K., *J. Non-Cryst. Solids*, 8 (1972), 293.
[37] ALMOND D.P., WEST A.R., *Nature*, 306 (1983), 456.
[38] MURTHY L.C.S., RAO K.S., *Bull. Mater. Sci.*, 22 (1999), 953.
[39] MUKHERJEE A., MITRA P., *Mater. Sci.-Poland*, 33 (2015), 847.
[40] GUO Z.J., JIANG H.Y., YONG C.S., XIAO D.X., BIAO P., *Acta Phys. Pol. A*, 115 (2009), 944.
[41] ALAEDDIN A.S., POOPALAN P., *J. Mater. Sci. Technol.*, 27 (2011), 802.
[42] MURAWSKI L., BARCZYNSKI R.J., *J. Non-Cryst. Solids*, 185(1995), 84.
[43] OUNI B., LAKHDAR M.H., BOUGHALMI M., LARBI T., BOUKHACHEM A., MADANI A., BOUBAKER K., AMLOUK M., *J. Non-Cryst. Solids*, 367 (2013), 1.
[44] TIWARI B., CHOUDHARY R.N.P., *J. Phys. Chem. Solids*, 69 (2008), 2852.
[45] PONCE M.A., CASTRO M.S., ALDAO C.M., *J. Mater. Sci. Mater. El.*, 20 (2009), 25.

Received 2016-08-11
Accepted 2017-06-28